

See discussions, stats, and author profiles for this publication at: <https://www.researchgate.net/publication/12328153>

# Uncompensated resistance. 2. The effect of reference electrode nonideality

ARTICLE *in* ANALYTICAL CHEMISTRY · OCTOBER 2000

Impact Factor: 5.64 · DOI: 10.1021/ac000154x · Source: PubMed

---

CITATIONS

8

---

READS

55

## 2 AUTHORS:



**Keith Oldham**

Trent University

**272** PUBLICATIONS **8,590** CITATIONS

SEE PROFILE



**Nicholas Stevens**

The University of Manchester

**44** PUBLICATIONS **443** CITATIONS

SEE PROFILE

# Uncompensated Resistance. 2. The Effect of Reference Electrode Nonideality

Keith B. Oldham\* and Nicholas P. C. Stevens<sup>1</sup>

Department of Chemistry, Trent University, Peterborough, Ontario, Canada K9J 7B8

**A finite-element simulation study has been made of the effect upon the uncompensated resistance,  $U$ , of the size of a reference electrode positioned at various distances above the center of an inlaid-disk working electrode. The idealized reference electrode is treated as a conducting circular disk embedded in a cylindrical insulator. Two effects are encountered, in addition to the expected diminution in  $U$  as the reference electrode approaches the working electrode. A “backwater effect”, reducing  $U$ , arises from the avoidance of the Luggin probe by the current lines. A “short-circuiting” effect, enhancing  $U$ , arises if those current lines pass through the reference electrode on their way to the counter electrode. Two detrimental effects of the intrusion of a finite-sized reference electrode into the vicinity of the working electrode—a reduction in the total current and the perturbation of the current density distribution—are also briefly examined. It is demonstrated that  $U$  may be reduced indefinitely by decreasing the working-to-reference gap, but, the Luggin probe must have a diameter of one-fourth or less of that of the working electrode if significant shielding is to be avoided.**

Concern for uncompensated cell resistance has been shown ever since the invention of the potentiostat<sup>2</sup> permitted electrochemical cells to be operated unencumbered by the total cell resistance. Interest has heightened of late because of the increasing attention that electrochemists are paying to systems of low conductivity. The purpose of the present modeling study is to investigate quantitatively how geometric factors influence the uncompensated resistance. Inevitably, the study resorts to idealizations.

The passage of a faradaic current  $I$  through a voltammetric cell from the working electrode WE to the counter electrode CE generates an array of equipotential surfaces in the electrolyte solution. If the potential of the solution in immediate contact with the working electrode is accorded the value  $\phi_W = 0$  then, by Ohm's law, the layer of solution adjacent to the counter electrode will have the potential  $\phi_C = -RI$ , where  $R$  is the total cell resistance. Note that the potential  $\phi$  anywhere in the solution away from WE will be negative if  $I$  is positive, i.e., if the electrode reaction is anodic. In a typical three-electrode voltammetric experiment, a potentiostat enforces a potential on the working

electrode that differs from that of a reference electrode RE by some predetermined (and often time-dependent) value. To prevent uncertainty in the interfacial potential at the working electrode, one would like there to be no potential difference at all between the electrolyte solution that bathes WE and that which contacts RE. To come close to this ideal, the reference electrode commonly incorporates a so-called Luggin capillary consisting of a thin conductor sheathed by an insulator. The uninsulated tip of this Luggin probe is placed in solution in close proximity to the surface of the working electrode. In this location, the RE's tip will intersect one of the equipotential surfaces, say that one having the value  $\phi_R$ . In fact, the entire conducting surface of the RE will adopt this potential. In these terms, the “uncompensated resistance”  $U$  is the fraction of the total cell resistance given by

$$\frac{U \phi_W - \phi_R}{R \phi_W - \phi_C} = \frac{\phi_R}{\phi_C} \quad (1)$$

Stated differently but equivalently,  $U$  is the resistance of the column of solution that separates the entire equipotential surface at  $\phi_R$  from the working electrode. The uncompensated resistance is linked to the current and to the conductivity  $\kappa$  of the solution (assumed constant and uniform) by the equations

$$U = \frac{R \phi_R}{\phi_C} = \frac{-\phi_R}{I} = \frac{1}{g\kappa} \quad (2)$$

where  $g$  is a factor, having the dimensions of a length, that is determined by the geometry of the cell and its three electrodes.

The factors that constitute the geometry of the cell and that therefore conjoin to determine the value of  $g$ , and hence establish the uncompensated resistance  $U$ , include the following items: (i) the size and shape of the cell; (ii) the size and shape of WE; (iii) the size and shape of CE and the CE/WE interelectrode spacing; (iv) the RE/WE gap and the angular relation of RE to the CE/WE axis; (v) the size and shape of RE's tip and of the Luggin's sheath. Though, of course, the coverage was less than comprehensive, the first four of the listed items were addressed in part 1 of this study.<sup>3</sup> To lessen the number of factors bearing on the problem, the investigations of items i–iv were carried out for an “ideal” reference electrode. In the present context, an ideal RE is one whose sole pertinent property is position; it has neither size

(1) Present address: Department of Chemistry, Monash University, Clayton, Vic 3168, Australia.

(2) Hickling, A. *Trans. Faraday Soc.* **1942**, 38, 27.

(3) Myland, J. C.; Oldham, K. B. *Anal. Chem.*, preceding article in this issue.

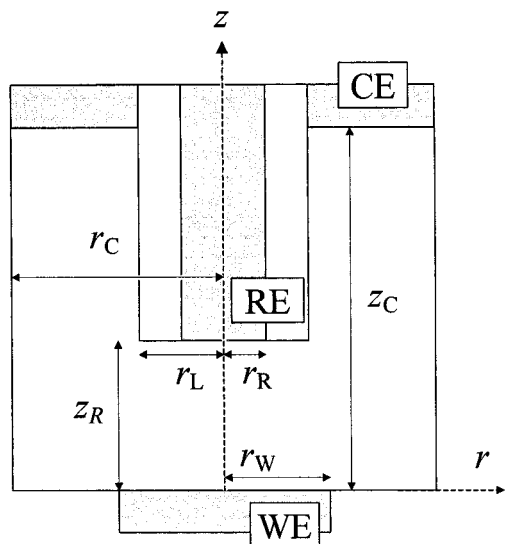


Figure 1. Idealized cell on which our modeling is based. All three electrodes are disks, parallel to each other, and centered on the symmetry axis  $r = 0$  of the cell. Of course, this diagram is not to scale. In our simulations  $r_C$  and  $z_C$  exceeded  $r_W$  100-fold.

nor shape. This ideal is approached as the width of the Luggin probe is progressively diminished.

In practice, any reference electrode has at least two other geometric attributes in addition to its position with respect to WE: the size of the conductor's tip and the width of the insulating sheath. The dependence of  $U$  on these factors, and upon the gap separating RE from WE, is addressed in this article. Just as part 1 adopted an ideal reference electrode while investigating the role of other cell components, so in part 2 we shall idealize aspects i–iv of the cell geometry, so as to better isolate the role of RE's size and shape, as well as its distance from WE. The only cell geometry we consider is that illustrated in Figure 1. The working electrode is an inlaid disk of radius  $r_W$ , whose center is the origin of the  $(r, z)$  cylindrical coordinate system we adopt. The counter electrode is a remote plane, distance  $z_C$  from WE. By "remote" we mean that  $z_C$  is so large that making it larger still would have no significant effect on  $U$ . The cell width,  $2r_C$ , which also determines the diameter of CE, is "effectively infinite" in size, by which is meant that  $U$  would not be significantly changed by increasing  $r_C$  still further. Though studies in part 1 suggest that much more conservative values would suffice, we set  $z_C = r_C = 100r_W$  in our modeling. We consider the center of the reference electrode to lie on the  $r = 0$  symmetry axis of the cell, with the RE/WE gap being denoted  $z_R$ . Various sizes are accorded to the radius<sup>4</sup>  $r_R$  of the conducting core of the reference electrode and to the overall width (core + sheath)  $2r_L$  of the Luggin capillary. Only flat-ended probes are treated, though rounded or tapered probes are not uncommon in experimental practice.

When the reference electrode is "ideal", it has only one quality of importance: the degree of resistance compensation that it delivers. The less  $U$  is the better; there are no detrimental effects from an ideal RE. This is not the case with reference electrodes of finite size. The space occupied by RE is space that would

otherwise be occupied by solution, and therefore, the distributions of potential and current are modified from what they would have been in the absence of the reference electrode. This secondary effect, the blockage of the current path, is termed "shielding" and is investigated in later sections of this article. Shielding is potentially harmful because, within our knowledge, the presence of the reference electrode is never taken into account in modeling the voltammetric process. Accordingly, false conclusions may be drawn by interpreting experimental data that has been unwittingly corrupted by shielding, even though the troublesome resistance may be efficiently minimized or even completely eliminated by some procedure such as positive feedback<sup>5</sup> or measure-and-simulate.<sup>6</sup> We discuss shielding later in this article. Not only is the total current affected by an RE of finite size but the distribution of current density at WE is also affected. The final section briefly touches on this effect later.

Working voltammetric electrodes that are not uniformly accessible invariably suffer current density dispersion. By this is meant that certain regions of WE support a higher current density than other regions. For example, the current density at an inlaid disk electrode is least at the center of the disk and greatest at its periphery, where the current density may even be infinite.<sup>7,8</sup> Moreover, the current density dispersion changes with time, in a way that also depends on the reversibility of the electrode reaction. As a result, the locations of the equipotential surfaces change with time, so that the uncompensated resistance, and other features associated with the reference electrode, including shielding, suffer time dependence. These time-dependent effects will be ignored here, but they are considered in part 3 of this series of articles.

To set the stage for discussion of the uncompensated resistance for a cell designed as in Figure 1, we report the result for an *ideal* reference electrode. The exact mathematics in part 1 of this study leads to the conclusion that the equation

$$U_{\text{ideal}} = \arctan\{z_R/r_W\}/2\pi r_W \kappa \quad (3)$$

provides a simple expression for the uncompensated resistance when both  $r_R$  and  $r_L$  are negligibly small. Note that by setting  $z_R = \infty$  in this equation, we correctly generate the expression

$$R = 1/4r_W \kappa \quad (4)$$

for the total cell resistance.<sup>9</sup> Notice also that, when  $z_R$  and  $r_W$  are equal, eq 3 predicts that  $U_{\text{ideal}}$  will equal  $1/8r_W \kappa$ , exactly half of the total cell resistance  $R$ .

## METHOD OF CALCULATION

Rather than reporting calculated values of  $U$  itself, it is more useful to cite values of the dimensionless group  $Ur_W \kappa$ , because this avoids having to assign arbitrary values to the radius  $r_W$  of the inlaid disk and the conductivity  $\kappa$  of the electrolyte solution. Our investigation of RE nonideality, then, will provide numerical values of  $Ur_W \kappa$  as a function of three ratios of the four pertinent

(4) The same  $r_R$  symbol was used in part 1 to symbolize, not the radius of RE, but its radial position. There should be no confusion because the latter quantity is invariably zero in part 2.

(5) Roe, D. K. In *Laboratory techniques in electroanalytical chemistry*; Kissinger, P. T., Heineman, W. R., Eds.; Dekker: New York, 1996.

(6) Bond, A. M.; Oldham, K. B.; Snook, G. *Anal. Chem.*, **2000**, 72, 3492–3496.

(7) Newman, J. *Electrochemical Systems*; Prentice Hall: Englewood Cliffs, NJ, 1973; Section 117.

(8) Oldham, K. B.; Zoski, C. G. *J. Electroanal. Chem.* **1988**, 256, 11.

linear dimensions:

$$U_{RWK} = f\{z_R, r_R, r_L, r_W\} = f\left\{\frac{z_R}{r_W}, \frac{r_R}{r_W}, \frac{r_L}{r_W}\right\} \quad (5)$$

When  $r_R/r_W = r_L/r_W \rightarrow 0$ , to take the simplest nontrivial example, eq 3 shows that  $U_{RWK} = (1/2\pi) \arctan\{z_R/r_W\}$  and this analytical result provided data for the dashed lines in Figures 2, 4, and 7 that follow later in this article.

In essence, the calculation of uncompensated resistance requires the solution of Laplace's equation, which is

$$\nabla^2 \phi = \frac{\partial^2 \phi}{\partial z^2} + \frac{\partial^2 \phi}{\partial r^2} + \frac{1}{r} \frac{\partial \phi}{\partial r} = 0 \quad (6)$$

in the cylindrical coordinates ( $z, r$ ) of our system, subject to the boundary conditions

$$\phi(z=0, r < r_W) = \phi_W = 0, \quad \text{by definition} \quad (7)$$

$$\phi(z=z_C, r < r_C) = \phi_C = \text{a known (negative) constant} \quad (8)$$

$$\phi(z=z_R, r < r_R) = \phi_R = \text{an a priori unknown constant} \quad (9)$$

and to the requirement that the equipotential surfaces intersect all the insulating boundaries of the cell orthogonally. The solution provides the locations of *all* equipotential surfaces, but the prime interest is in identifying  $\phi_R$ . Note that the assumed high conductivity of the Luggin's core implies that the electrolyte solution in contact with the entire conducting surface of RE shares the same potential  $\phi_R$ , even when  $r_R$  is large.

Of course, the rate of passage of charge across each equipotential surface is the total current  $I$ , and this fact can be used to evaluate  $I$ . The most convenient site for this evaluation is the surface of WE, so that

$$I = -2\pi\kappa \int_0^{r_W} r \left( \frac{\partial \phi}{\partial z} \right)_{z=0} dr \quad (10)$$

The uncompensated resistance is then found via eq 2, by dividing  $-\phi_R$  by  $I$ .

In part 1, we relied on algebraic formulas to provide numerical values, but the geometry of the cell in Figure 1 is too complicated for our mathematical skills and we have therefore resorted, as have others<sup>10</sup> previously, to finite element modeling. Details of our finite element solution of the Laplace equation, and of how this enables the current lines to be located, have been relegated to Supporting Information.

#### EFFECT OF THE WIDTH OF THE LUGGIN PROBE

In the present section, the conducting core of the Luggin probe is taken to have an infinitesimal thickness, as it had in part 1 of this study. Unlike the geometry of part 1, however, this core is sheathed by an insulator of finite width so that, in terms of the dimensions inscribed in Figure 1,  $r_R \ll r_L$ , the latter not being insignificant compared to the radius  $r_W$  of the working electrode or the interelectrode gap  $z_R$ . In these circumstances, the normalized uncompensated resistance  $U_{RWK}$  depends on two factors

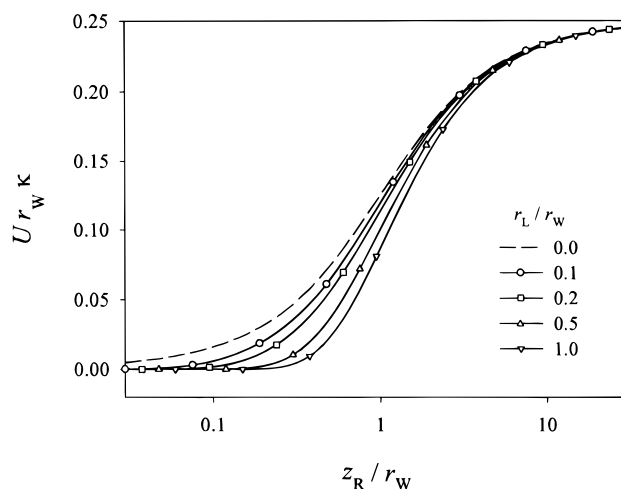


Figure 2. Graphs of the normalized uncompensated resistance  $U_{RWK}$  as a function of the distance  $z_R$  separating the reference and working electrodes, normalized by division by  $r_W$ . The symbol key shows, for each curve, the ratio  $r_L/r_W$  of the radii of the Luggin probe to that of the working electrode. The dashed line corresponds to an ideal reference electrode of infinitesimal size and is based on eq 3; all other curves are based on finite-element simulations. The thickness of the conducting tip of RE is negligible for this graph.

only: the ratio  $z_R/r_W$  of the interelectrode gap to the radius of WE and the ratio  $r_L/r_W$  of the radius of the Luggin capillary to that of the working electrode disk. We have simulated this geometry to determine the uncompensated resistance for ranges of these two ratios.

Figure 2 shows the results of our simulation as a plot of  $U_{RWK}$  versus  $z_R/r_W$ , the latter being plotted logarithmically. The number associated with each curve is the radius ratio  $r_L/r_W$ . Each curve shows the effect of varying the interelectrode gap, and they all exhibit a decline in uncompensated resistance as the gap is diminished. This effect, which we term "the proximity effect", is well appreciated by experimentalists who routinely endeavor to place RE as close as possible to WE. Notice in Figure 2 that RE is behaving almost ideally, as evidenced by the closeness of the curves to the dashed line, whenever  $r_L/r_W$  is sufficiently small or  $z_R/r_W$  is sufficiently large. Observe, however, that there is a marked decrease in  $U$  as the radius of the Luggin increases, especially when  $z_R$  is small. For example, when  $z_R = 0.5r_W$ , the uncompensated resistance halves as the Luggin radius increases from 0.1 to  $0.5r_W$ .

Data similar to those in Figure 2 are presented differently in Figure 3. Here each curve relates to a specific constant interelectrode gap and the Luggin radius appears on the logarithmic abscissa. Note the expected approach of  $U$  to  $0.25/r_{WK}$  at large WE/RE separation, as  $U \rightarrow R$ , the *total* cell resistance, which eq 4 shows to equal  $1/4r_{WK}$ . Figure 2 shows clearly that little compensation is achieved unless RE is closer to WE than the radius of the latter. Each curve displays a sigmoidal shape, emphasizing the drop in  $U$  attributable to the "backwater" effect—the diminished ohmic drop across the interelectrode gap caused by the current, on its way to the counter electrode, having to avoid the impediment that the Luggin probe represents. The left-hand plateaus, corresponding to sheath radii of less than  $\sim 5\%$  of the working disk's radius, obey eq 3 exactly, signifying ideality. The right-hand plateaus are attained when  $r_L$  exceeds about twice  $z_R$ ,

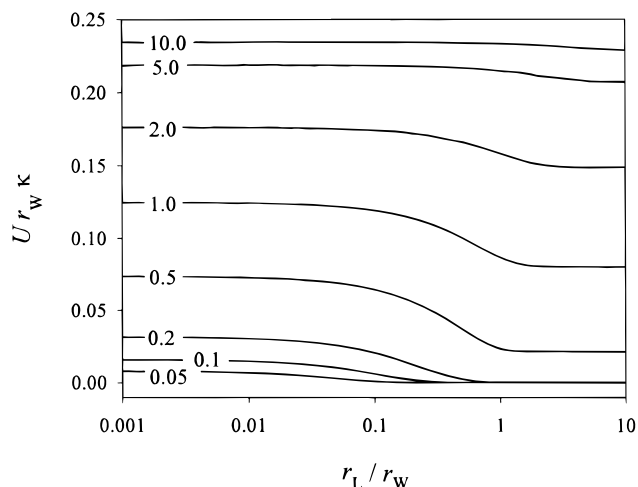


Figure 3. Data similar to those in Figure 2 replotted to demonstrate the sigmoidal behavior of  $U$  as a function of the Luggin radius. The number associated with each curve is the ratio  $z_R/r_W$  of the interelectrode gap to the radius of the working electrode.

so that the Luggin completely blocks all normal access to the solution from WE, a situation unlikely to occur in voltammetric practice, except perhaps in poorly designed microelectrode experiments.

#### EFFECT OF THE RADIUS OF THE REFERENCE ELECTRODE'S CONDUCTOR

In this section, we discuss simulations to determine how the finite size of the reference electrode affects the uncompensated resistance when the insulating sheath is of negligible thickness. Thus, we set  $r_R \approx r_L \gg (r_L - r_R)$ . Experimentally, this condition could be realized when the Luggin probe is a lacquered metal wire.<sup>11</sup>

Figure 4 shows the results of these simulations as a plot of  $U_{RW\kappa}$  versus the logarithmically scaled ratio  $z_R/r_W$  for a variety of  $r_R/r_W$  radius ratios. For values of the radius ratio less than  $\sim 0.5$ , the curves closely mirror those in Figure 2 and exhibit the expected decline in uncompensated resistance as the interelectrode gap decreases and the serendipitous diminution in  $U$  as  $r_R$ , and therefore, the total probe radius  $r_L$ , increases. This can be attributed to a backwater effect.

Though the range  $r_R < 0.5r_W$  will cover most macroelectrode experiments, we nevertheless pursued the interesting effect that occurs as the radius of RE becomes comparable with, and overtakes, that of WE. As is evident in Figure 4, the uncompensated resistance then increases, often surpassing the ideal resistance indicated by the dashed line. The cause of this curious behavior can be understood from Figure 5, in which the current lines and equipotential surfaces are mapped for the case  $r_R = z_R = 2r_W$ . It is evident that part of the current avoids a crowded path through the resistive electrolyte solution, by a "short circuit" route

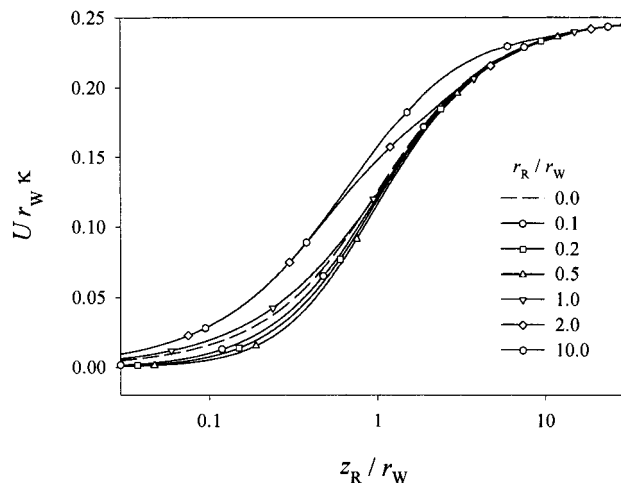


Figure 4. Graphs of the normalized uncompensated resistance  $U_{RW\kappa}$  versus the normalized interelectrode gap. The symbol key gives the ratio  $r_R/r_W$  of the radii of the two electrodes (or equivalently the ratio  $r_L/r_W$ ). The dashed line corresponds to an ideal reference electrode of infinitesimal size. The thickness of the insulating sheath of the reference electrode is negligible for this figure, as it is in Figures 5 and 6 also.

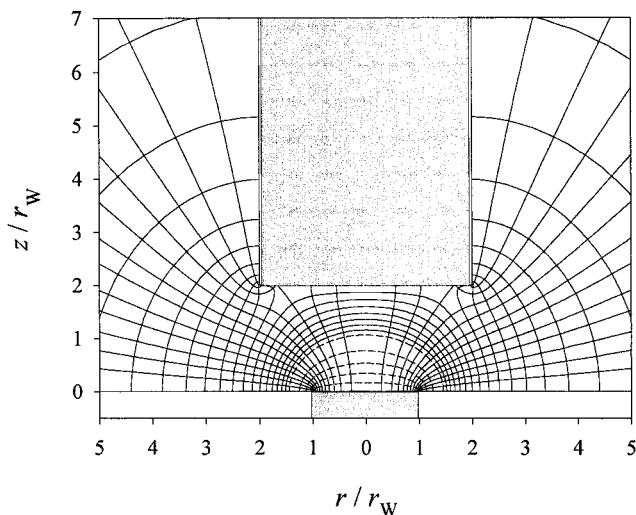


Figure 5. Illustration of the current lines emanating from the working electrode when  $r_L \approx r_R = z_R = 2r_W$ . The dashed lines represent equipotential surfaces; their spacing is  $\phi_C/10$  close to WE and  $\phi_C/40$  further out. In this case, 20% of the current short-circuits through the reference electrode.

through RE's core.<sup>12</sup> The uncompensated resistance thus increases on account of the enhanced current flow in the interelectrode gap.

The twin effects of the "backwater" and the "short-circuit" are more clearly seen in Figure 6, which is analogous to Figure 3, except that, for clarity, both axes are here scaled logarithmically. The increase in uncompensated resistance that occurs over the range  $0.5r_W < r_R < 1.5r_W$  is seen to be dramatic, often exceeding 10-fold. A geometry that leads to such a massive effect as this would be unlikely to arise in conventional electrochemical practice; however, it could occur in microelectrode studies if RE is placed

(9) Newman, J. J. *Electrochem. Soc.* **1966**, 113, 1235.

(10) Winkler, J.; Hendriksen, P. V.; Bonanos, M.; Mogensen, M. *J. Electrochem. Soc.* **1998**, 145, 1184.

(11) Such a lacquered wire would transfer the potential  $\phi_R$  to its other end. This could be immersed in a sample of the cell solution housed in a separate vessel equipped with a conventional reference electrode (an SCE, for example), so providing thorough depolarization.

(12) The extent to which this occurs in practice will depend on the relative conductivities of the two media and on the facility with which electricity can cross the interface. Our modeling assumes a worst case scenario: RE's core is infinitely conductive and the interface imposes no barrier to the passage of current.



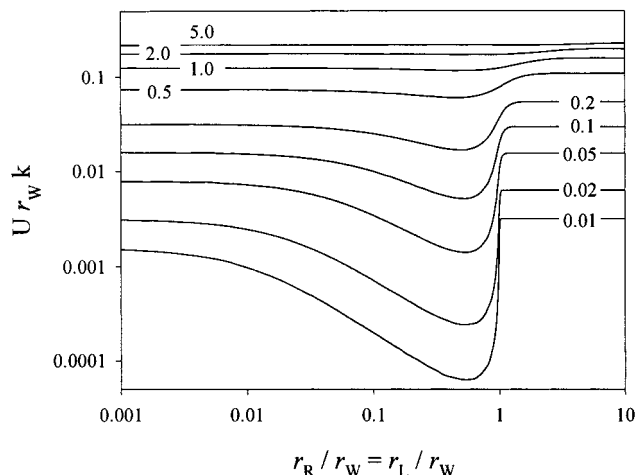


Figure 6. Graphs of the normalized uncompensated resistance  $U r_W \kappa$  versus the ratio  $r_R / r_W$  of the radii of the two electrodes, both axes being scaled logarithmically. The number associated with each curve is  $z_R / r_W$ , the interelectrode distance normalized by the radius of WE.

incautiously close to WE. The sudden change in  $U$  at  $r_L = r_W$ , especially when  $z_R$  is small, can be understood readily because, as  $r_L$  increases beyond  $r_W$ , direct access from WE to the bulk solution is abruptly cut off. It is easy to appreciate why the effect is so dramatic when one realizes that 50% of the total current from a steady-state inlaid disk arises from the rather narrow circumferential annulus  $0.87 r_W < r \leq r_W$ . This fact is a straightforward consequence of eq 14 below.

#### EFFECT OF BOTH THE CORE AND THE SHEATH BEING IMPORTANT

The previous two sections addressed the uncompensated resistance when either  $r_R$  or  $r_L - r_R$  was small enough to be ignored. In experimental practice, however, the radius of RE and the width of the Luggin sheath are often of comparable magnitude. Accordingly the graphs in this section address uncompensated resistances and current distribution for a "fifty-fifty" electrode, when  $r_L = 2r_R$ , so that half of the radius (and one-fourth of the area) of the Luggin is conductor, and half insulator.

As might have been predicted, the behavior when the conductor and the sheath contribute equally to the radius of the Luggin is intermediate between those described in this paper. Invariably we observe the proximity effect, the uncompensated resistance increasing, as Figure 7 illustrates, as the interelectrode gap widens, and approaching the total cell resistance  $1/4 r_W \kappa$  at large separations. The behavior as a function of the Luggin radius is more interesting. For a small enough Luggin probe, say  $r_L$  less than 2% of  $r_W$ , the reference electrode behaves almost ideally, closely following eq 3. As the  $r_L$  increases,  $U$  progressively declines in response to the backwater effect, the fall being especially pronounced when the interelectrode gap is small. For larger values of the  $z_R / r_W$  ratio, such as that shown in Figure 8, the Luggin capillary distorts the current flow only marginally and the uncompensated resistance is only 5% smaller than the ideal value. The effect on the current lines of increasing the Luggin size, for a given interelectrode gap, is seen by comparing Figure 9 with Figure 8. A 3-fold increase in  $r_L$  has been accompanied by an extensive distortion of the current lines. Interestingly, almost the

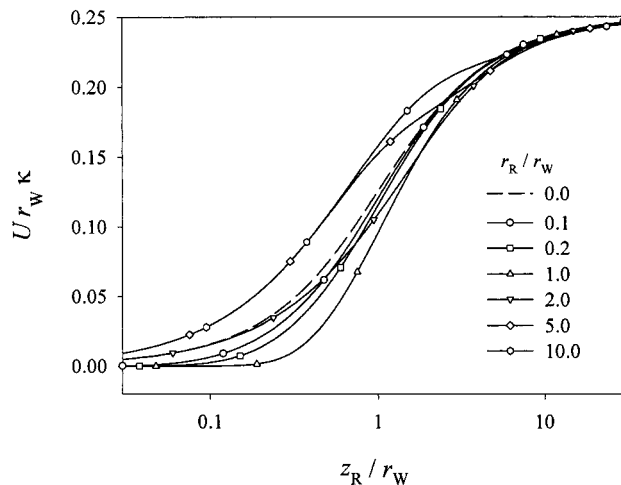


Figure 7. Graphs of the normalized uncompensated resistance  $U r_W \kappa$  as a function of  $z_R / r_W$ , the interelectrode gap normalized by division by  $r_W$ . The abscissa is plotted logarithmically. The thickness of the Luggin sheath is equal to the radius of the conducting core of RE for this graph and for Figures 8–10, 13, and 14. The number associated with each curve in this figure is the ratio  $r_R / r_W$  of the radii of the Luggin probe to that of the working electrode, or equivalently  $r_L / 2r_W$ . The dashed line corresponds to an ideal reference electrode of infinitesimal size.

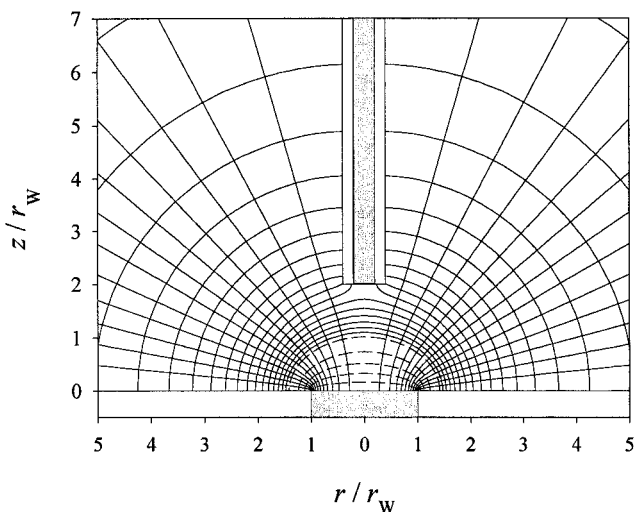


Figure 8. Current lines and equipotential surfaces for the "fifty-fifty" case  $z_R = 2r_W = 5r_L = 10r_R$ . Notice that there are only small departures of the equipotential surfaces from the oblate spheroids (which degenerate toward hemispheres at greater distances) that would exist in the absence of the reference electrode.<sup>22</sup> Accordingly, the current lines are only slightly distorted, too.

same uncompensated resistance ( $0.11 / r_W \kappa$ ) is associated with Figure 9 as with Figure 8. The increasing backwater effect has been compensated by a small short-circuit effect.

The presence of short-circuiting is evidenced by the telltale increase in  $U$ , in Figure 10 as  $r_R$  overtakes  $r_W$ . This figure is a graph of the uncompensated resistance versus Luggin size for cases in which the width of the Luggin's insulation matches the core radius. Notice that the transition to the higher  $U$  values occurs as  $r_R$ , not  $r_L$ , surpasses  $r_W$ . This confirms that the sudden increase in  $U$  is a result of the short-circuiting effect and is not caused by a simple blanketing of the working electrode by the Luggin capillary.

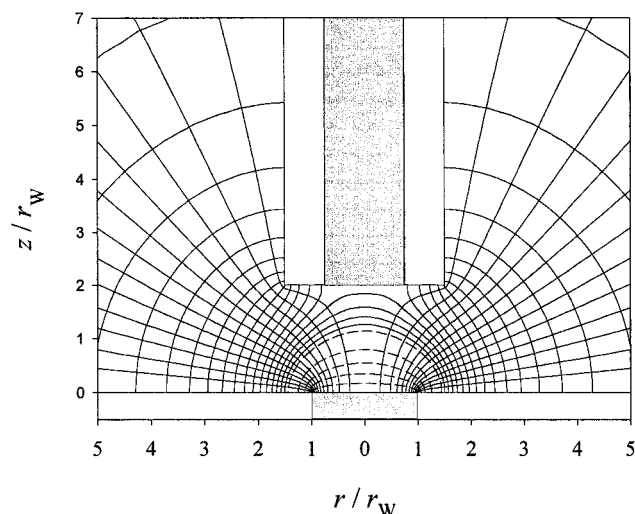


Figure 9. Current lines and equipotential surfaces for another fifty-fifty case  $z_R = 2r_W = 4r_L/3 = 8r_R/3$ . Please note the much greater distortions here than in Figure 8. Though it is not evident in the current lines, there is appreciable short-circuiting occurring in this geometry. The spacing of the equipotential surfaces in Figures 8 and 9 is as explained for Figure 5.

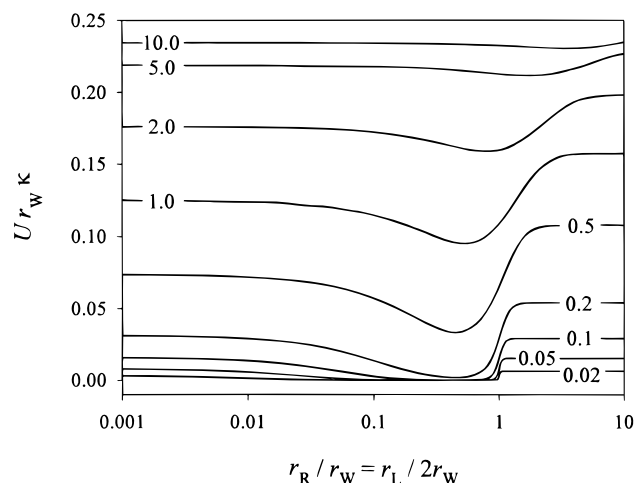


Figure 10. Graphs of the normalized uncompensated resistance  $U r_W \kappa$  versus the ratio  $r_R/r_W$ , plotted logarithmically. The number associated with each curve is  $z_R/r_W$ , the interelectrode gap divided by the core radius of WE.

Unfortunately, if the size of the Luggin probe is not insignificant compared with that of working electrode, voltammetry may be affected other than via changes in the uncompensated resistance. These other effects are detrimental to voltammetric performance. If the presence of RE has a significant effect either on the total current  $I$  or on the current density distribution across ( $r \leq r_W$ ,  $z = 0$ ), the face of WE, then the model with which the experimental voltammogram is to be compared may be compromised or totally invalidated. Shielding and current density perturbation are two ways in which such an invalidation may arise. They are addressed in the following sections.

#### DEFINITION OF SHIELDING

"Shielding" as we use the term here, must be distinguished from another, somewhat similar, phenomenon that may be encountered when a reference electrode is too close to the

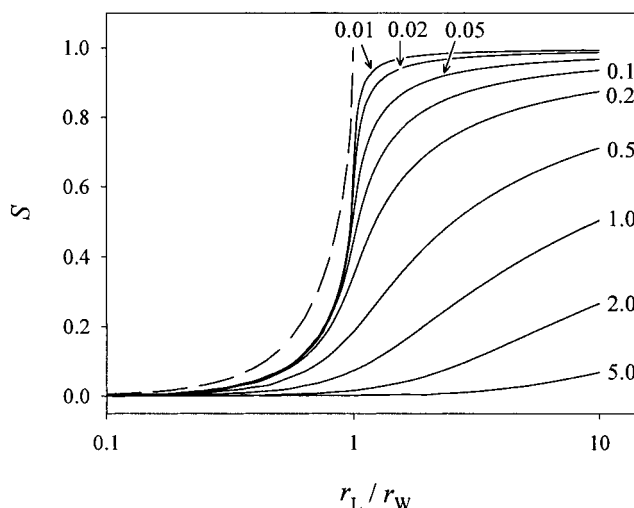


Figure 11. Graphs of  $S$ , the degree of shielding, versus the ratio of the radius of the Luggin probe to the radius of the inlaid disk, for the case of negligible  $r_R$ . The number associated with each curve is the normalized interelectrode gap,  $z_R/r_W$ . The dashed line gives an upper limit to  $S$  according to eq 14.

working electrode. When an electrode is working faradaically, it is surrounded by a "transport layer" in which the concentration of the electroreactant and/or electroproduct is significantly different from that in the bulk of the electrolyte solution. For example, in a simple diffusion-controlled chronoamperometric experiment (a "Cottrell experiment") in which the potential is stepped, at time  $t = 0$ , to a value at which complete concentration polarization of the planar electrode occurs, the concentration of the electroreactant at a distance  $z$  from WE is diminished by a factor  $\text{erfc}\{z/2(Dt)^{1/2}\}$  from its bulk value.<sup>13</sup> For the typical magnitude,  $D = 1 \times 10^{-9} \text{ m}^2 \text{ s}^{-1}$  of the diffusivity, and after 1 min of polarization, this factor reaches 15% for  $z = 0.5 \text{ mm}$ . Clearly, if the WE/RE gap is only 0.5 mm in such an experiment, and if the Luggin has an appreciable size, it will begin to interfere seriously with the natural growth of the transport layer after  $\sim 60 \text{ s}$ , thereby affecting the current. Moreover, the mixture of reactant and product may exert a Nernstian effect on the potential of an RE of the "quasi-reference" variety. We call these effects "transport layer penetration". They are likely to be encountered only in abnormally lengthy voltammetric experiments, and especially in steady-state studies at microelectrodes. Transport layer penetration is also an important consideration in hydrodynamic voltammetry,<sup>14</sup> where transport layers are often unusually wide. We propose to ignore transport layer penetration here.

Shielding arises from the nonideality of the reference electrode, being absent if the Luggin is vanishingly small. When there is no RE, or only a minutely sized RE, current can flow unimpeded or almost unimpeded between WE and CE. The physical presence of a finite sized Luggin will block some of the routes between the working and counter electrodes and thereby alter (usually diminish) the current  $I$ . This is the effect that we call "shielding". Shielding is detrimental because it corrupts the current, a quantity from which chemical conclusions are routinely drawn following

(13) Brett, C. M. A.; OliveraBrett, A. M. *Electrochemistry: Principles, Methods and Applications*; Oxford University Press: Oxford, U.K., 1993; p 87.

(14) Yet another important consideration in hydrodynamic voltammetry is the interference that RE may cause to the hydrodynamic regime.

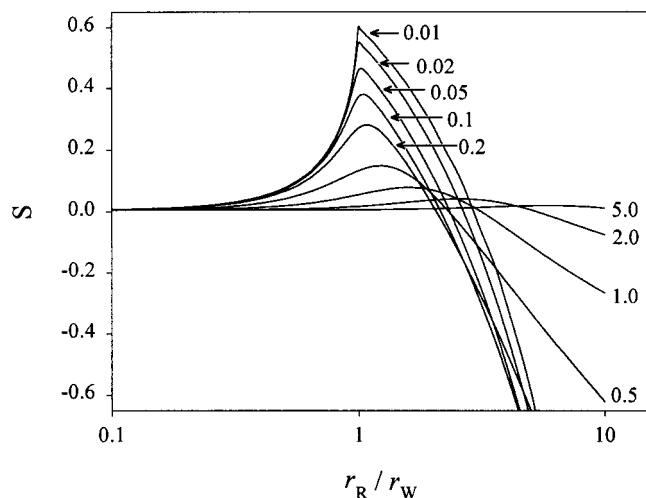


Figure 12. Degree of shielding as a function of the normalized radius of the reference electrode. The number associated with each curve is the ratio  $z_R/r_W$  of the interelectrode gap to WE's radius. These graphs apply when  $r_L \approx r_R$ , that is, when there is an infinitesimally thick insulating sheath on the Luggin probe.

a voltammetric experiment. It will also change the distribution of current density at the working electrode, as exemplified later. We might expect that it is the WE/RE gap and the overall size of the Luggin probe, characterized by  $r_L$ , that are important in affecting shielding, with  $r_R$  being relatively unimportant. This is generally true, but the occurrence of the short-circuiting can play a role in mitigating the effects of shielding, even, in extreme conditions, reversing the sign of the effect.

#### MAGNITUDE OF THE SHIELDING EFFECT

In the absence of shielding, as guaranteed if there is no reference electrode at all, the current flowing in a cell of the design shown in Figure 1 is

$$I_{\text{ideal}} = -\phi_C/R = -4r_W\kappa\phi_C \quad (11)$$

where  $\phi_C$  is the potential of the solution layer adjacent to CE with respect to the corresponding layer in contact with WE. The "degree of shielding"  $S$  may be defined as the fractional decrease in the total current caused by shielding resulting from the physical presence of the reference electrode. Thence, using eqs 10 and 11, we have

$$S = \frac{I_{\text{ideal}} - I}{I_{\text{ideal}}} = 1 - \frac{\pi}{2r_W\phi_C} \int_0^{r_W} r \left( \frac{\partial \phi}{\partial z} \right)_{z=0} dr \quad (12)$$

Because the same integral was used en route to the evaluation of the uncompensated resistance, only trivial additional calculations are needed to determine the degree of shielding from our simulations.

It might be conjectured that the degree  $S$  of shielding cannot exceed that corresponding to the total blockage of that portion of WE lying directly under RE. The current density  $i$  at an unimpeded inlaid disk electrode is the function<sup>9,15,16</sup>

$$i = I/2\pi r_W \sqrt{r_W^2 - r^2} \quad (13)$$

Table 1. Minimum Distance of Approach of a Fifty-Fifty Luggin Probe (i.e., One with  $r_L = 2r_R$ ) to a Working Electrode To Avoid Significant (i.e., >2%) Shielding and the Corresponding Uncompensated Resistance<sup>a</sup>

$r_L/r_W$	$z_R/r_W$	$U/R$	$r_L/r_W$	$z_R/r_W$	$U/R$
<0.25	0.00	0.00	0.70	1.32	0.53
0.28	0.24	0.06	0.80	1.43	0.57
0.30	0.36	0.12	0.90	1.51	0.60
0.35	0.56	0.22	1.00	1.58	0.63
0.40	0.73	0.29	1.50	1.81	0.72
0.50	1.02	0.41	2.00	1.93	0.77
0.60	1.19	0.48			

<sup>a</sup>The latter is expressed as a fraction of the total cell resistance  $R$ .

of the radial position  $r$ , where  $I$  is the total current. Therefore, our conjecture leads to the prediction that

$$S < 1 - \frac{2\pi}{I} \int_0^{r_L} r i dr = 1 - \frac{1}{r_W} \sqrt{r_W^2 - r_L^2} \quad (14)$$

The dashed line in Figure 11 represents that conjecture.

Figure 11 shows the degree of shielding as a function of the radius ratio  $r_L/r_W$ , for various values of the normalized interelectrode gap. This figure is for the case when  $r_R \approx 0$ , so that short-circuiting is inhibited. Evidently the conjecture represented by the dashed line is correct. It is also evident, as expected, that shielding becomes severe as the radius of the Luggin approaches that of the working electrode, especially for small interelectrode spacings. If we set 2% as the degree of shielding that can be tolerated, then the maximum allowable radius of the Luggin probe is as reported in Table 1.

This tabulation shows how close (in terms of  $z_R/r_W$ ) the reference electrode may approach WE without incurring unacceptable shielding. The corresponding extent of resistance compensation is also listed. For example, with a 5.0-mm-diameter inlaid disk electrode, a reference electrode with Luggin radius of 1.0 mm can be brought within 1.8 mm of the disk's center without causing significant shielding; 71% of the resistance would be compensated in that position. Our simulation shows that only if  $r_L < 0.25r_W$  can the reference probe be brought indefinitely close to the disk's center without appreciable shielding. This is to be compared with the  $r_L < 0.20r_W$  predicted by the more stringent eq 14.

Short-circuiting was impossible for the configurations to which Figure 11 relates, but it is prevalent in those to which Figure 12 applies. The enhanced current caused by short-circuiting counteracts shielding and can lead to a degree of shielding that is nominally negative. Again, these interesting effects are likely to be encountered experimentally only in unusual circumstances.

How a reference electrode that is too close almost shuts off the current from the portion of WE that lies beneath it is shown in Figure 13. In the case illustrated, there is virtually no current at all from the central region of the working electrode.

#### PERTURBATION OF THE CURRENT DENSITY

Equation 13 gives the current density distribution  $i_{\text{ideal}}$  appropriate to an unimpeded inlaid disk working electrode in the



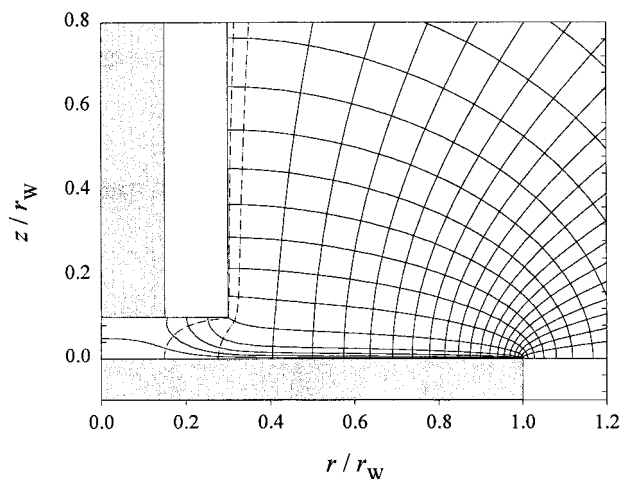


Figure 13. Current lines and equipotential surfaces for the fifty-fifty case when  $r_L = 2r_R = 3r_W/10$  and  $z_R = r_W/10$ . Inside the leftmost dashed line, only 0.1% of the total current flows, even though it originates from 2.3% of WE's area. Likewise the 1% of the total current that flows in the zone between the two dashed lines arose in an annular zone representing 3.4% of the working electrode's area.

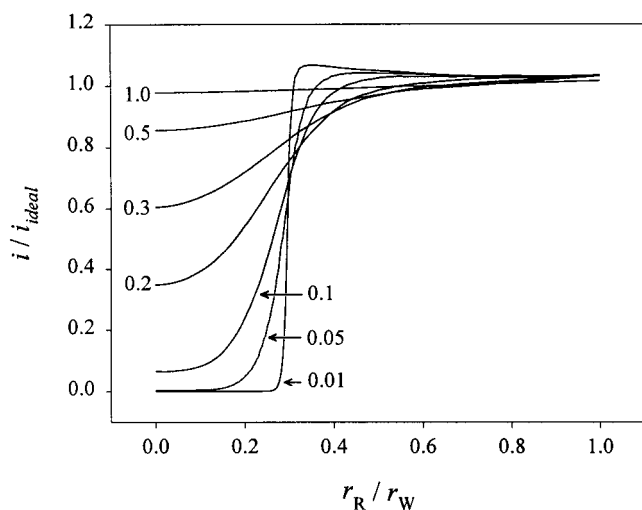


Figure 14. Current-density profiles, normalized by the ideal profile given by eq 13, for the case  $r_L = 2r_R = 3r_W/10$ . The number attaching to each curve is the value of  $z_R/r_W$ .

steady state. How is that distribution affected by the presence of a nearby reference electrode? Figure 14 answers that question for the case when  $r_L = 2r_R = 3r_W/10$ . Several different interelectrode gaps are represented by the different curves, which show the actual distribution of current density divided by the ideal current density predicted by eq 14. Note that it is not until  $z_R$  is as large as  $r_W$  that the current density distribution approaches ideality.

(15) Nanis, L.; Kesselman, W. *J. Electrochem. Soc.* **1971**, *118*, 454.

(16) Oldham, K. B. *J. Electroanal. Chem.* **1989**, *260*, 461.

(17) If the wire lacks an insulating sheath, the effect could be worse still.

## CONCLUSIONS

We conclude that there are three factors affecting the uncompensated resistance, and that they are general: (i) The proximity effect, reflecting the value of  $z_R$ . This is the well-known property that the closer RE is to WE, the smaller is  $U$ . (ii) The backwater effect, reflecting the value of  $r_L$ . The larger the diameter of the Luggin probe is, the more the current avoids the region in front of RE, decreasing the uncompensated resistance. (iii) The short-circuit effect, reflecting the value of  $r_R$ . The larger the size of the conducting core of RE, the more does it provide a conductive path en route to CE. This counteracts effect ii, by encouraging current flow close to the axis, and may overwhelm it, so that  $U$  can exceed  $U_{\text{ideal}}$ .

It should be stressed that the magnitude of effect iii depends not only on  $r_L$  but also on the conductivity of the Luggin's core. Here we have treated only the worst case—that in which the core's conductivity is infinite. This would be apt when a so-called "pseudoreference" is used in the form of a metal wire.<sup>17</sup> The short-circuit effect will occur with a "salt bridge" type of reference electrode also, but will be less severe than in the examples given here.

Whenever one strives for a high degree of compensation, shielding will be a severe limitation unless it is taken into account or Luggin probes are restricted in radius to one-quarter or less of that of WE. The effects of current-density perturbation may be important, even when shielding is not.

We have only addressed reference electrodes positioned directly in front of the center of the working disk electrode. As demonstrated in part 1,<sup>3</sup> this is the optimal position as far as resistance compensation is concerned. From the viewpoint of shielding, too, a central location for RE is optimal because the current density is minimal along  $r = 0$ .

## ACKNOWLEDGMENT

The financial support of the Natural Sciences and Engineering Research Council of Canada is acknowledged with gratitude, as is the award of a Research Fellowship to N.P.C. Stevens by the U.K. Royal Society of Chemistry.

## SUPPORTING INFORMATION AVAILABLE

(A) Finite element solution of the Laplace equation; (B) location of current lines. This material is available free of charge via the Internet at <http://pubs.acs.org>.

Received for review February 7, 2000. Accepted June 5, 2000.

AC000154X